T. Schneider (Editor)/*Acidification and its Policy Implications*
Elsevier Science Publishers B.V., Amsterdam - Printed in The Netherlands

TRAJECTORY MODELS OF THE LONG-RANGE AIR POLLUTANT TRANSMISSION

A.J.Pressman, M.V.Galperin and J.E.Mikhailova
Meteorological Synthesizing Centre-East, EMEP (USSR)

While modelling the long-range and transboundary air pollutant transmission it is usually necessary to identify sources responsible for deposition at a given area. The problem solution being formulated in such way can be easily made by simulation of the history of pollutant plumes in the variable wind fields.

First let us consider point source (Fig. 1) at constant wind. For simplicity the wind direction is assumed to be coincident with positive direction of x axis. Let us keep track of a single pollutant puff emitted by a source during infinitely short time interval at t = 0. Using a known sollution from the semi-empirical turbulent diffusion theory: the concentration at the location with co-ordinates x = r, y = ℓ at z height is obtained from

$$\tilde{c}\ (r,\ \ell,\ z,\ t) = (2\pi\sigma_r\sigma_\ell)^{-1}\ \exp\ [-\frac{(r-Vt)^2}{2\sigma_r^2} - \frac{\ell^2}{2\sigma_\ell^2}]\ \Psi\ (z,\ t) \qquad (1)$$

where t = time, σ = pollutant dispersion along the plume, σ_ℓ = dispersion in the transverse direction, V = wind speed, and function Ψ (z,t) describes vertical distribution of pollutant depending on time and conditions of absorbtion at the earth surface.

Other processes of pollutant removal from the air (e.g. chemical transformation and wash-out) do not impact on the spatial distribution since as to first approximation they may be considered to be volumetrical effects. Therefore it is possible to study eq. (1) without factors describing these processes.

It is shown in |2| that a sufficiently large-scale pollutant distribution (just in case of long-range transmission) the diffusion in wind direction may be ignored, i.e. $\sigma_r \to 0$. Due to known characteristics we have Dirac δ-function |12|:

$$\lim_{\sigma_r \to 0}\ \frac{1}{\sigma_r\sqrt{2\pi}}\ \exp\ [-\frac{(r-Vt)^2}{2\sigma_r^2}]\ = \frac{1}{V}\ \delta\ (\frac{r}{V} - t) \qquad (2)$$

Putting (2) into (1) we obtain

$$c\ (r,\ \ell,\ z,\ t) = (2\pi\ V\sigma_\ell)^{-1}\ \exp\ (-\frac{\ell^2}{2\sigma_\ell^2})\ \delta(\frac{r}{V} - t)\ \Psi\ (z,\ t) \qquad (3)$$

Formula (3) characterizes the concentration distributions along ℓ and z in "infinitely thin" puff's in x = r direction. Fig. 1 (curve 1) shows horizontal pollutant distribution in such a puff at distance r from the source, and Fig. 2 - the shape of Ψ (z) function characterizing the vertical pollutant distribution.

Note that the source is continuous and assuming source emission to be constant and equal to Q_s it is possible to determine the concentration at fixed state ($t \to \infty$). Due to properties of δ-function

$$c\ (\frac{r}{V},\ \ell,\ z) = \int_0^\infty Q_s\ \tilde{c}\ (r,\ \ell,\ z,\ t)\ dt = Q_s(\sqrt{2\pi}\ V\sigma_\ell)^{-1}\exp(-\frac{\ell^2}{2\sigma_\ell^2})\ \Psi(z,\ \frac{r}{V}) \qquad (4)$$

The transformation can be described in the form (Fig. 1):if the source is continuous then an infinitely great number of puff's that do not exchange material ($\sigma_r = 0$) are located along x = r. Each puff is depleted at every time step and pollution distribution is changed within. At the same time the puff is transported in V direction (and therefore in r) leaving the place for the next puff. However, due to stationary conditions a new puff at any point x = r will have the same features as previous one. Thus the pollutant concentration depends on Q_s, V, $\frac{r}{V}$, ℓ and z and it doesn't depend on time t.

The role of t (absolute time) is transmitted to another parameter of the same dimension as t that is age of a given puff:

$$\tau = \frac{r}{V} \qquad (5)$$

In view of (5) from (4) it follows that the pollution flux through the plane orthogonal to x and crossing it a point x = r is

$$Q_c\ (\tau) = V\int_0^\infty \int_0^\infty c(\tau,\ell,z)\ d\ell dz = Q_s\int_0^\infty \Psi(z,\tau)\ dz \qquad (6)$$

Thus function

$$\zeta_d\ (\tau) = \int_0^\infty \Psi(z,\tau)\ \ dz \qquad (7)$$

characterizes the pollutant fraction remaining in the atmosphere τ-time after emission. In other words function $\zeta_r(\tau)$ is a function of pollutant removal by dry deposition. Integrating the expression for $\Psi(z,\tau)$ |8| for weightless pollutants we obtain

$$\zeta_d(\tau) = \mathrm{erf}(\frac{h}{2\sqrt{K_z\tau}}) + \mathrm{erfc}\frac{h+2V_d\tau}{2\sqrt{K_z\tau}}\ \exp\frac{V_d h + V_d^2\tau}{K_z} \qquad (8)$$

where V_d= dry deposition velocity, depending on the pollutant type, K_z = vertical turbulent diffusion coefficient, h = source height.

Introduction of parameter τ allows for volumetric processes of removal, chemical transformation and wash-out. On the assumption that these processes can be described by usual linear differential equations of the first order we obtain as wash-out function:

$$\zeta_w(\tau) = \exp(-\Lambda J^{\alpha} \tau) \tag{9}$$

where precipitation intensity $J(x,y,t)$ depends on co-ordinates x,y and real time t, and parameters Λ and α depend on pollutant type and the function for chemical transformation:

$$\zeta_T(\tau) = \exp(-\lambda_T \tau) \tag{10}$$

where λ_T = coefficient of chemical transformation of SO_2 to SO_4^{2-}. Here and further all the values are concerned with oxidized sulphur independent of the compound (SO_2 or SO_4^{2-}). Designating by indices 1 and 2 values of SO_2 and SO_4^{2-} we can write full functions of removal for SO_2

$$\zeta_1(\tau) = \zeta_{1d}(\tau)\ \zeta_{1w}(\tau)\ \zeta_T(\tau) \tag{11}$$

and conservative pollutant - sulphates

$$\zeta_2(\tau) = \zeta_{2d}(\tau)\ \zeta_{2w}(\tau) \tag{12}$$

In view of (11) and (12) for SO_2 and sulphate fluxes we have

$$Q_{1c}(\tau) = Q_s\, \zeta_1(\tau) \tag{13}$$

$$Q_{2c}(\tau) = \lambda_T Q_s \int_0^{\tau} \zeta_1(\nu)\ \zeta_2(\tau - \nu)\, d\nu \tag{14}$$

The above relationships from the basis of an analytical approach of model development based on the simulation of plume history in a variable wind field. The fact that pollutant amount in a puff is utterly determined by its age allows to use the above considerations when wind speed is varied in direction and module (Fig. 3). One should, however, adequately consider diffusion in ℓ direction.

Let us consider the process of plume generation and transport on the whole. Let at t moment the plume projection on x,y plane be at position 1 (Fig. 3). We assume that the wind filed {V} is stationary within Δt time interval. The puff generated by t will be shifted to position 2 for $\Delta\tau$ time. In this time period a new puff is generated. At any point ($\sigma_r = 0$) diffusion in the plume will be taken as orthogonal to its axis. The plume "is not aware" that it is curvilinear and locally it behaves as if it were rectilinear and tangent to its axis. On the basis of numerous experimentel data for Gaussian distribution ℓ direction (see (4)) we assume

$$\sigma_{\ell} \cong 0.1\ r \tag{15}$$

where r = full plume axis length. The Gaussian distribution is approximated as uniform at final interval $\pm\ \ell$, thus

$$|\ell| = 2\sigma_{\ell} \tag{16}$$

where $|\ell|$ = plume half-width. Thus while constructing the plume it can be assumed that at a first approximation horizontal diffusion is proportional to the plume length r and is determined by expressions (15) and (16) (line 2 in Fig. 1).

Now we should choose values for the basic parameters of relationships (8)-(10).

Dry deposition velocities (V_d) for sulphur compounds in MSC-E models were taken from |5|, obtained by statistical analysis of |9| and information provided by Co-ordinating Chemical Centre (CCC) EMEP |11|

$$V_{d\ SO_2} \cong 50\ m\ h^{-1}\ ; \qquad V_{d\ SO_4^{2-}} \cong 10\ m\ h^{-1}\ ;$$

CCC's data processing shows that on the average over Europe in January-February V_d is decreased (about 0.6 of mean annual value) and in April and October-November V_d exceeds mean annual value by as much as 1.2-1.3 times. K_z varies with seasons. The mean value of $1.10^4\ h^{-1}$ K_z is decreased to about $10^4\ m^2\ h^{-1}$ in January-February and it is increased to $10^5\ m^2\ h^{-1}$ in July-August.

For pollutants with long lifetime (sulphates, in particular) function (8) with limited τ avoiding appreciable lowering of the accuracy can be approximated by dependence

$$\zeta_{2d}(\tau) \cong \exp(-\lambda_{2d}\tau) \tag{17}$$

where $\lambda_{2d} \cong \pi V_{2d}^2/Kz \cong 0.01\ h^{-1}$ for sulphates. Such an approximation doesn't lead to great errors with $\tau > 1/\lambda_d \cong 100$ h. Pollution transmission over Europe is occuring 100-120 hours (nearly equal to sulphate lifetime). Approximation (17) allows us to simplify calculations of sulphate dry deposition since it follows from (17) that the fraction of sulphates resulted from dry deposition does not depend on τ at short time interval Δt and its equal to $\lambda_{2d}\Delta t$.

For wash-out (see (9)) at the first approximation $\alpha = 1$ may be assumed then $\Lambda = 0.4\ mm^{-1}$ for one-layer model and sulphur compounds. This value was obtained through regression analysis of data on SO_2 and sulphate wash-out |11|.

Precipitation data from the meteorological network (WMO) is processed in MSC-E. All the meteorological stations that provide information for the period in question are scatted in grid squares and mean value for pollutant fraction after wash-out remaining in the air is determined for each square by (9)

$$\bar{\zeta}_w = \frac{1}{M} \sum_{i=1}^{M} \exp(-\Lambda J \Delta t) \qquad (18)$$

where M = number of stations in a given square. Correspondingly washed out pollutant fraction in a square is $(1 - \bar{\zeta}_w)$.

Chemical transformation coefficient $SO_2 \rightarrow SO_4^{2-}$ λ_T (see (10)) is assumed to be dependent on season |5|

$$\lambda_T \ [\% \ h^{-1}] \cong 1.7 - \cos[\pi (n-1)/6]$$

where n = number of a month in the year.

For the simulation of transport information a real wind field is used. Synoptic wind and geopotential information provided by meteorological network stations is processed before its application in calculations |10|. Data of upper air measurements (not forecast) not only increase the calculation accuracy but allow us to take into account the orographic effect on transmission of pollutants.

Now let us consider discrete-analytical simulation models of a trajectory type for long-range and transboundary transport of sulphur comounds based on the approach set forth above |6,7|.

MSC-E uses models of several types aimed at the solution of two problems: (a) calculation of pollutant fluxes across a given border with identification of sources contributing to fluxes crossing a given border segment; (b) calculation of concentration and deposition fields on the scale of a continent and determination of the contribution of a source to deposition at a given area. Calculation of "emitter-receiver matrices" is a particular case of the latter problem.

The EMEP territory is covered by a grid (gridsize 150 x 150 km). Each grid square is considered to be an elementary pollutant source and/or an elementary pollutant receiver. For modelling purposes it is necessary to have integral emission values for such squares.

To calculate fluxes across assumed borders in the model, the pollutant plume axis is constructed on the basis of wind data. In every time interval Δt at the centre of square-emitter with co-ordinates x_o, y_o control point portion is generated transporting to the location with co-ordinates:

$$x_1 = x_o + u_o \Delta t \ ; \qquad y_1 = y_o + v_o \Delta t \qquad (19)$$

where u_o and v_o are wind components at the source. Each puff that leaves the source has as its position

$$x_{n+1} = x_n + u_n \Delta t \ ; \qquad y_{n+1} = y_n + v_n \Delta t$$

in accordance with u_n and v_n in points x_n, y_n. At the same time the number of each puff is increased by 1. By consecutive connection of puff centres beginning with the source the broken line represents the plume axis at time t. In order to limit the plume length (at $t \to \infty$ $n \to \infty$) it is assumed in the model that at $n > N$, where N is a quantity assumed in advance, the plume is depleted and the track of its continuation is not kept. In view of the fact that meteorological information field is changed in a discrete way every 6 hours, time step $\Delta t = 6$ and $N = 16$ (maximum $\tau = 96$ h) are assumed.

Horizontal plume expansion at a certain point is determined by relationships (15) and (16). In view of horizontal expansion each plume segment is transformed into a trapezium-like segment with Δr_n height equal to plume axis segment at which the segment is constructed and with bases $2\ell_{n-1} = 0.4\ r_{n-1}$ and $2\ell_n = 0.4\ r_n$ with $\Delta r_n = r_{n-1}$. It is assumed that pollutant is uniformly distributed with segment area equal to $0.2\ (r_n^2 - r_{n-1}^2)$.

For each plume segment area we calculate acoording to (8), (10) and (18) the pollutant fraction remaining in the atmosphere after dry and wet deposition and chemical transformation. The calculation results can be used in two ways. First there is information on the pollutant flux crossing border contours. Note that the plume can cross the border more than once and the model is able to fix both direct and returned fluxes. Second the described scheme was successfully used for deposition and concentration calculations [7]. Segments at discontinuity points should be reconstructed in a proper way. That is the angle formed by plume axis segments is divided by the bisector. Correspondingly plume segment area's are increased on the convex side and decreased on the concave one. In the model presented, surface concentrations are calculated by formulea resulting from (6) and (17)

$$c_{1g} = Q_{1c}(\tau)\ \Psi_1(0,\tau)\ \frac{1}{s\zeta_{1d}(\tau)}\Delta t \tag{20}$$

$$c_{2g} = Q_{2c}(\tau)\ [\lambda_{2d}/(V_{2d}s)]\ \Delta t \tag{21}$$

where s = area under plume segment. Dry (D) and wet (W) deposition are determined from the relationships

$$D = c_g V_d \tag{22}$$

$$W = \frac{1}{s} Q_c(\tau)\ (1 - \sum_j \overline{\zeta}_{wj})\ \Delta t \tag{23}$$

where j = number of squares with centres covered by segment, Δt = time step. Sulphate formation at each step Δt is simulated by

$$\Delta Q_{2c} = \lambda_T Q_{1c}(\tau)\ \Delta t \tag{24}$$

The approach of model development for deposition and concentration calculations can be improved. Using the segment plume construction, the consideration of asymmetry resulting from non-uniform wash-out of pollutant from segment area makes the calculation very difficult. Here the calculation is simplified but there is a possibility to make more accurate consideration of wash-out in the model based on the dynamics of individual puff's with finite area.

Contrary to |4| in the last version of MSC-E model initial puff's have a square shape corresponding to an emitter of 150 x 150 km^2. Every hour each emitter generates a puff with a pollutant amount equal to that of hourly emission. This puff is transported and expanded conforming with data on real wind field independent of other puff transmission from this or any other source. Designate the puff centre at t_n time to be co-ordinates x_n, y_n and their linear dimensions along Cartesian axes X_n and Y_n. By analogy with (15), (16) and (19) it is assumed that

$$x_{n+1} = x_n + \bar{u}_n ; \tag{25}$$

$$y_{n+1} = y_n + \bar{v}_n ; \tag{26}$$

$$X_{n+1} = X_n + 0.4\,\bar{v}_n \tag{27}$$

$$Y_{n+1} = Y_n + 0.4\,\bar{u}_n \tag{28}$$

Here $\bar{u}_n$ and $\bar{v}_n$ are the mean weighted vector components of wind speed or the transmission velocity, the derivation of which is described below.

When the puff is in x_n, y_n and determined by its Length X_n, Y_n, changes in its composition are estimated by (24). Grid square centres covered by the puff are determined and dry and wet deposition are calculated from equations

$$D_n = \left[-m_{1n}\,\frac{1}{\zeta_{1d}(\tau)}\,\frac{d}{d\tau}\,\zeta_{1d}(\tau) + m_{2n}\,\lambda_{2n}\right]\frac{\Delta t}{k_n} \tag{29}$$

$$W_j = \frac{m_n}{k_n}\,(1 - \bar{\zeta}_{wj}) \tag{30}$$

where m_{1n} and m_{2n} = sulphur amount (as SO_2 and SO_4^{2-} respectively) in the puff k_n = number of squares covered by puff, ζ_{wj} is obtained from eq. (18). It is assumed that initially the pollution is uniformly distributed within all the squares which centres are covered. After dry and wet deposition over the j-th square pollutant, an amount $m_j = m_{j1} + m_{j2}$ is left and the total pollutant amount is

$$m_n = \sum_{j=1}^{k} m_j$$

where k = number of squares covered. Hence mean wind components at $t_n = n\Delta t$ are derived with allowance for contributions of individual squares

$$\bar{u}_n = \sum_{j=1}^{k} u_j m_j / m_n ; \qquad \bar{v}_n = \sum_{j=1}^{k} m_j v_j / m_n \tag{31}$$

These values are used for the calculations of the puff centre co-ordinates after the (n+1)-th step from (25) and (26) and its size lengths from (27) and (28).

Since the puff is identified with sources as well as with square-receivers "emitter-receiver matrices" are compiled simultaneously with deposition calculations.

The puff's history is detected when three conditions are met:

(a) puff's age $\tau < 120$ hours;

(b) total puff's amount exceeds known value PD (it is usually assumed PD = 0.5; 1; 2 t);

(c) puff's centre is located within the calculated grid.

If one of conditions (a) or (b) is violated then calculations are stopped and the remaining pollution amount is added to PVP value (background). The stored PVP value at the end of calculations for 24 hours is partially distributed within all the squares (background deposition from undecided sources) and partially this amount is considered to have left the calculated grid. Violation of conditions (c) leads to adding its total amount to PFB.

Thus the model provides the budget of emission and deposition and pollutant amount leaving the calculated region. In order to eliminate "failure" in the consideration of sources of low strength in case of violating condition (b), the adding to PVP and calculation ceasing is permitted only for puff's with $\tau > 1$ hour.

Calculations for 24 hours are made consecutively for all the puff's of one plume (one source) and then for all the plumes. In case calculations have to be stopped parameters of all the puff's which are initial conditions for new calculations are stored.

As a result of these consecutive calculations of all the plumes for 24 hours output tables of dry and wet deposition in squares and "emitter-receiver matrices" are provided.

After diurnal deposition calculations are completed, mean diurnal surface concentration c is determined from:

$$c_1 = D_{1\Sigma} / V_{1d} ; \quad c_2 = D_{2\Sigma} / V_{2d}$$

and the concentration in precipitation (W = deposition through precipitation):

$$c_p = W_\Sigma / J$$

for each grid square. Index "Σ" in these formulae shows the usage of integral deposition in a given square, and J = actual diurnal precipitation amount in each square.

The presented models have been tested by calculations of fluxes, deposition and concentrations and the results were compared with field measurements.

Verification of the flux model was made on the basis of aircraft measurements [1]. The results are presented in Table 1. For comparison only 10 flights were available during calculated months. This resulted in a bias in sulphate data.

In spite of the bias mentioned it is obvious that the agreement between calculated and measured concentrations in flux is quite satisfactory.

A more representative comparison is the one in which CCC data of mean monthly concentrations are compared with deposition model calculations.

To compare calculated sulphur concentrations at the surface with measured ones, a yearly period (October 1980 - September 1981) was chosen, since at the time of calculation, available data [11] for this period were the most comprehensive ones. Stations with known mean monthly concentrations higher than the background (about 0.5 mg S/m^3 for SO_4^{2-}) and with few gaps in time series (absence of data was accepted for not more than for 3 days) have been chosen.

Results of mean correlation coefficient values r and regression equations (Y = calculated, X = measured values) are presented in Table 2. Note that on the whole the agreement between calculated and measured data is worse in summer because of the lower stability of the atmosphere.

Nevertheless Tabel 2 indicates that the calculated results provide quite acceptable mean monthly concentration values. Relative mean root - square error of calculations relative to measured values:

$$\delta = \sqrt{\Sigma (c_c - c_m)^2 / \Sigma c^2_m}$$

where c_c and c_m = are calculated and measured concentrations of SO_2 and SO_4^{2-} respectively

$$\delta_{SO_2} = 0.16 \qquad \text{and} \qquad \delta_{SO_4^{2-}} = 0.23$$

The ratios of calculated and measured mean monthly values stay within the range of 0.5 - 2.0 with 99% probability for SO_2 en 95% probability for SO_4^{2-} (if we assume normal distribution of error). The inaccuracy range is 3.5 times smaller for mean annual values. In view of the problems set forth this result is statisfactory enough. Model calculations can give representative estimates of the long-range transboundary transmission of air pollution.

REFERENCES

1 Abramovskaya S.D., et al. Resultaty samoletnykh izmerenij transgranichnykh potokov soedinenij sery. Trudy Instituta Prikladnoj Geofiziki, 1985, vyp. 62, s.64-70, Moskva, Gidrometeoizdat.

2 Karol I.L. O vlianii turbulentnoj diffuzii v napravlenii vetra na raspredelenie kontstentratstii, diffundirujushchej v atmosfere. - Doklady AN SSSR, 1960, tom 131, N 6, str. 1283-1286.

3 Eliassen A. The OECD Study of Long-Range Transport of Air Pollution, Long-Range Transport Modelling.- Atm.Environ., 1978, v.12, N 1, p.28-40.

4 Ellenton G., Ley B., Misra P.K. A Trajectory Puff Model of Sulfur Transport for Eastern North America.- Atm.Environ., 1985, v.19, N 5, p.727-737.

5 Galperin M.V. O smeshchenii otstenok soderzhaniya primesej v atmosfere obuslovlennom statisticheskimi fluktuatstiyami skorostey vyvedeniya.- Meteorologiya i Gidrologiya, 1984, N 4, s.23-31.
(On the shift of estimations of pollutant content in the atmosphere caused by statistical fluctuations of removal rates).

6 Izrael Yu.A., Mikhailova J.E., Pressman A.J. Model dlya operativnoy otstenki transgranichnykh potokov antropogennykh primesey. - Doklady AN SSSR, v.253, N 4, 1980, c.848-852.

7 Mikhailova J.E. Model dlya otstenki vklada krupnykh istochnikov v transgranichnoe zagryaznenie atmosfery i mestnosti soedineniyami sery v masshtabakh kontinenta.- Trudy IPG, 1982, vyp.48.

8 Monin A.S. Trudy Geofizicheskogo Instituta AN SSSR, N 33, 1956.

9 Sehmel G.A. Particle and Gas Dry Deposition: a review.- Atm.Environ., 1980, v.14, N 9.

10 Shapiro M.Ya. Objektivnij analiz polya vetra na osnovanii dannykh o geopotentstiale i vetre.- Trudy IPG., 1982, vyp. 62, str.59-64.

11 Skielmoen T.E., Schang T., Data report October 1980 - September 1981.- NILU EMEP/CCC, Report 6/84, Lillestrøm, 1984, 452 p.

12 Van der Pol B., Bremmer H. Operational Calculees based on the two-sided Laplace integral.- Cambridge, Univer, Press, 1950.

TABLE 1

Comparison of aircraft concentration measurements (mg/m^3) and model calculation of fluxes

Parameter	SO_2		SO_4	
	Calculated	Measured	Calculated	Measured
Mean value	3.51	3.85	3.27	3.1
Mean root-square deviation	2.75	3.1	1.07	1.43
Correlation coefficient r	0.83		0.74	
Regression equation (X - calculated concentration, Y - measured concentration)	Y = 0.93X + 0.6		Y = 0.98X - 1.17	

TABLE 2

Comparison of measured mean monthly concentration values of SO_2 and SO_4 with calculated results

Month, year	SO_2				SO_4			
	Mean		r	Regression equation	Mean		r	Regression equation
	Measured	Calculated			Measured	Calculated		
October 80	3.07	2.8	0.85	Y = 0.77X + 0.44	1.14	1.1	0.58	Y = 0.87X + 0.10
November 80	4.53	3.9	0.79	Y = 0.79X + 0.32	1.31	1.2	0.85	Y = 0.74X + 0.23
December 80	7.16	6.8	0.83	Y = 0.65X + 2.10	1.70	1.9	0.73	Y = 0.96X + 0.25
January 81	6.95	8.0	0.79	Y = 0.88X + 1.90	1.95	1.4	0.92	Y = 0.89X - 0.34
February 81	6.22	7.7	0.68	Y = 1.14X + 0.61	2.66	1.9	0.62	Y = 0.61X + 0.28
March 81	4.03	4.6	0.71	Y = 1.06X + 0.33	1.67	1.5	0.74	Y = 0.63X + 0.45
April 81	3.20	3.1	0.91	Y = 1.01X - 0.13	1.81	1.4	0.67	Y = 0.98X - 0.37
May 81	2.41	2.8	0.84	Y = 1.09X + 0.17	1.45	1.2	0.69	Y = 0.59X + 0.34
June 81	2.00	3.5	0.72	Y = 0.89X + 0.30	1.91	1.9	0.65	Y = 0.54X + 0.90
July 81	1.65	2.3	0.67	Y = 1.21X + 0.30	1.48	1.3	0.53	Y = 0.68X + 0.30
August 81	1.96	2.1	0.78	Y = 0.95X + 0.24	1.44	1.7	0.68	Y = 0.61X + 0.82
September 81	2.16	2.7	0.81	Y = 0.91X + 0.73	1.85	2.6	0.88	Y = 1.13X + 0.51
Total for year	3.85	4.2	0.89	Y = 1.03X + 0.23	1.70	1.6	0.83	Y = 0.94X + 0.00

Fig. 1

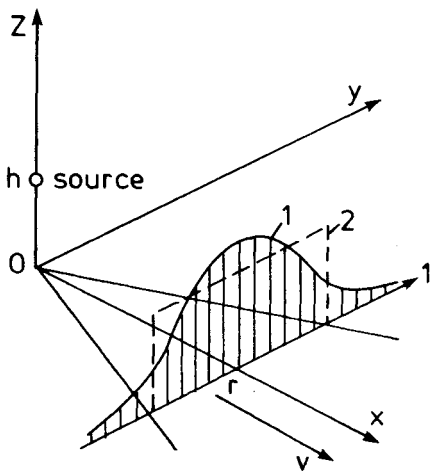

Fig. 2

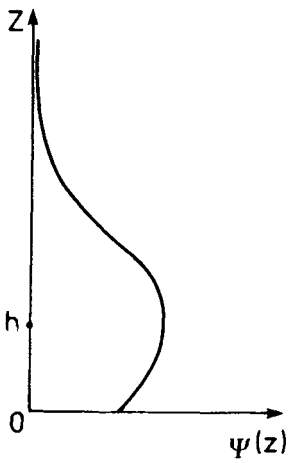

Fig. 3